Published in final edited form as:

Clin Cancer Res. 2018 June 01; 24(11): 2574–2584. doi:10.1158/1078-0432.CCR-17-2954.

Toxicity and Efficacy of a Novel GADD34-expressing Oncolytic HSV-1 for the Treatment of Experimental Glioblastoma

Hiroshi Nakashima[1], **Tran Nguyen**[1], **Kazue Kasai**[1], **Carmela Passaro**[1], **Hirotaka Ito**[1], **William F. Goins**[2], **Imran Shaikh**[3], **Ronald Erdelyi**[3], **Reiko Nishihara**[4], **Ichiro Nakano**[3], **David A. Reardon**[5], **Ana C. Anderson**[6], **Vijay Kuchroo**[6], **E. Antonio Chiocca**[1]

[1]Harvey W. Cushing Neuro-oncology Laboratories (HCNL), Department of Neurosurgery, Harvard Medical School and Brigham and Women's Hospital, Boston, Massachusetts

[2]Department of Microbiology and Molecular Genetics, University of Pittsburgh School of Medicine, Pittsburgh, Pennsylvania

[3]Department of Neurological Surgery, The Ohio State University, Columbus, Ohio

[4]Department of Pathology, Harvard Medical School and Brigham and Women's Hospital, Boston, Massachusetts

[5]Center for Neuro-Oncology, Dana-Farber Cancer Institute, and Brigham and Women's Hospital, Boston, Massachusetts

[6]Evergrande Center for Immunologic Diseases and Ann Romney Center for Neurologic Diseases, Harvard Medical School and Brigham and Women's Hospital, Boston, Massachusetts

Abstract

Corresponding Authors: E. Antonio Chiocca, Brigham and Women's Hospital, 75 Francis Street, Boston, MA 02115. Phone: 617-732-6939; Fax: 617-734-8342; EAChiocca@bwh.harvard.edu; and Hiroshi Nakashima, HNakashima@bwh.harvard.edu. Current address for I. Nakano: Department of Neurosurgery, University of Alabama at Birmingham, Birmingham, Alabama.

Authors' Contributions

Conception and design: H. Nakashima, A.C. Anderson, V. Kuchroo, E.A. Chiocca

Development of methodology: H. Nakashima, E.A. Chiocca

Acquisition of data (provided animals, acquired and managed patients, provided facilities, etc.): H. Nakashima, T. Nguyen, H. Ito, I. Shaikh, R. Erdelyi

Analysis and interpretation of data (e.g., statistical analysis, biostatistics, computational analysis): H. Nakashima, C. Passaro, I. Shaikh, R. Nishihara, V. Kuchroo, E.A. Chiocca

Writing, review, and/or revision of the manuscript: H. Nakashima, T. Nguyen, C. Passaro, H. Ito, W.F. Goins, D.A. Reardon, E.A. Chiocca

Administrative, technical, or material support (i.e., reporting or organizing data, constructing databases): H. Nakashima, K. Kasai, W.F. Goins, I. Shaikh, I. Nakano, V. Kuchroo, E.A. Chiocca

Study supervision: H. Nakashima, E.A. Chiocca

Disclosure of Potential Conflicts of Interest

H. Nakashima and E.A. Chiocca are listed as co-inventors on a provisional patent application on the actual virus construct: NG34, that is owned by Partners/Brigham and Women's Hospital. W.F. Goins is a consultant/advisory board member for Oncorus. D.A. Reardon reports receiving speakers bureau honoraria from Bristol-Myers Squibb, EMD Serono, Genentech, Merck, and Regeneron. A.C. Anderson reports receiving commercial research grants from and is a consultant/advisory board member for Potenza Therapeutics and Tizona Therapeutics. No potential conflicts of interest were disclosed by the other authors.

The costs of publication of this article were defrayed in part by the payment of page charges. This article must therefore be hereby marked *advertisement* in accordance with 18 U.S.C. Section 1734 solely to indicate this fact.

Note: Supplementary data for this article are available at Clinical Cancer Research Online (http://clincancerres.aacrjournals.org/).

Purpose—Glioblastoma (GBM) is the most common primary central nervous system cancer in adults. Oncolytic HSV-1 (oHSV) is the first FDA-approved gene therapy approach for the treatment of malignant melanoma. For GBM, oHSVs need to be engineered to replicate within and be toxic to the glial tumor but not to normal brain parenchymal cells. We have thus engineered a novel oHSV to achieve these objectives.

Experimental Design—NG34 is an attenuated HSV-1 with deletions in the genes encoding viral ICP6 and ICP34.5. These mutations suppress virus replication in nondividing brain neurons. NG34 expresses the human *GADD34* gene under transcriptional control of a cellular Nestin gene promoter/enhancer element, whose expression occurs selectively in GBM. *In vitro* cytotoxicity assay and survival studies with mouse models were performed to evaluate therapeutic potency of NG34 against glioblastoma. *In vivo* neurotoxicity evaluation of NG34 was tested by intracerebral inoculation.

Results—NG34 replicates in GBM cells *in vitro* with similar kinetics as those exhibited by an oHSV that is currently in clinical trials (rQNestin34.5). Dose–response cytotoxicity of NG34 in human GBM panels was equivalent to or improved compared with rQNestin34.5. The *in vivo* efficacy of NG34 against two human orthotopic GBM models in athymic mice was similar to that of rQNestin34.5, whereas intracerebral injection of NG34 in the brains of immunocompetent and athymic mice showed significantly better tolerability. NG34 was also effective in a syngeneic mouse glioblastoma model.

Conclusions—A novel oHSV encoding *GADD34* is efficacious and relatively nontoxic in mouse models of GBM.

Introduction

Glioblastoma (GBM) is the most common primary central nervous system cancer in adults (1). Therapeutic options are limited by GBM's genetic and phenotypic heterogeneity, its immune-evasive ability, and by the brain–blood barrier that limits effective passage of drugs and other agents (2, 3). In fact, the reported median survival from the time of GBM diagnosis remains at 15 months (1). A plethora of clinical trials strive to improve survival for patients with this formidable brain cancer (4, 5).

Clinical development of any agents depends on their safety and efficacy profile (6). In this context, GBM is particularly challenging because of its location within neural elements that are critical to human function and quality of life. We and others have investigated HSV-based anticancer bioagents, such as oncolytic HSV-1 (oHSV), that are directly cytotoxic to GBM cells but also replicate and amplify within infected GBM cells (7). Like all similar agents, one major limiting factor for the successful use of oHSV against GBM may relate to the potential neurotoxicity of this bioagent. To limit neurotoxicity, most oHSVs, including those in clinical trials and FDA approved, were engineered to introduce defects in the two endogenous copies of the viral $\gamma_1 34.5$ genes that encode ICP34.5. ICP34.5's function is pleiotropic in the viral life cycle, but it has been shown to be the cause for neurovirulence/neurotoxicity of the virus in the CNS (8, 9). Neurovirulence of ICP34.5 is associated with disruption of autophagic flux through the binding to Beclin-1, an essential autophagic gene, and oHSV (Δ68H-6) carrying a Beclin-1 binding domain-deleted *ICP34.5* gene was reported

to be relatively non-neurovirulent (10). However, deletion of *$\gamma_1$34.5* from oHSV also blocks other functions of ICP34.5, which enables effective translation of viral-encoded messages within the host cell. The infected cell attempts to fight against an HSV-1 replication by activating protein kinase R (PKR), which in turn leads to phosphorylation of the translation initiation factor eIF2α and ultimate translational shutoff of viral messages (11, 12). Viral ICP34.5 counteracts this cellular action by activating a protein phosphatase 1 (PP1) that dephosphorylates eIF2α allowing for continued translation of viral mRNAs (11, 13).

The replication of ICP34.5-mutant oHSVs is often limited and severely attenuated, even in tumor cells (8, 10). We previously engineered an oHSV, rQNestin34.5, where one copy of the *$\gamma_1$34.5* gene was reinserted into the genome of the ICP34.5-deleted mutant oHSV, but whose transcription was driven by the cellular nestin gene enhancer and the hsp68 promoter (8), rather than an endogenous viral promoter. The nestin gene is highly transcribed in GBM cells but not in normal adult neurons. Nestin-based transcriptional control thus restricts rQNestin34.5 propagation to GBM cells, while in normal cells that are infected by the oHSV, ICP34.5 is not expressed and the virus does not replicate well. rQNestin34.5 has undergone extensive preclinical testing in support of an Investigational New Drug (IND) application and is currently being tested in a phase I clinical trial in human patients with GBM.

Transcriptional leakage and even minimal functionality from the *hsp68* promoter in normal CNS neuronal cells, if the nestin enhancer is inactive, could potentially lead to production of a small amount of ICP34.5, possibly resulting in virus-induced neurotoxicity. The carboxyl (C)-terminus of ICP34.5 shares significant homology with the C-terminal GADD34 (PPP1R15A) domain responsible for dephosphorylation of eIF2α by association with PP1 (12, 14–17). GADD34 is upregulated in cells as part of the endoplasmic reticulum (ER) stress response to allow the cells to maintain essential cellular metabolism (18–20). However, GADD34 does not possess the beclin-1–binding motifs of ICP34.5 responsible for neurotoxicity or suppression of autophagy (21–23).

We thus reasoned that rQNestin34.5 could be reengineered by switching out ICP34.5 with its human ortholog, GADD34. Here we report that this novel GADD34-encoded $\gamma_1$34.5-null oHSV (designated as NG34) exhibits kinetics of viral replication and propagation similar to those of rQNestin34 in GBM cells. This translates to NG34's efficacy in human orthotopic GBM mouse models that was equivalent to that of QNestin34.5. Of further interest, neurotoxicity studies revealed that NG34 was significantly less neurovirulent than rQNestin34.5 in the brains of non-tumor-bearing HSV-1–susceptible mice. These studies thus imply that NG34 will increase the therapeutic window of ICP34.5-based oHSVs for cancer therapy.

Materials and Methods

Cell culture

Human U251 glioma cells and their derivative cell lines, human U87ΔEGFR were cultured from in-house frozen stocks, and 293FT was purchased from Thermo Fisher Scientific, and U2OS and African green monkey Vero kidney cells were purchased from ATCC. Murine

glioma GL261 cells were originally obtained from Dr. Mariano Viapiano (SUNY Upstate Medical University, Syracuse, NY; ref. 24). These cells were cultured as monolayers on adhesive culture dishes containing DMEM (Thermo Fisher Scientific) supplemented with 2% or 10% FBS (Thermo Fisher Scientific), 100 μg/mL penicillin/streptomycin (Thermo Fisher Scientific), and 10 mmol/L HEPES (Thermo Fisher Scientific) at 37°C in a humidified incubator maintained at 5% CO_2. For passaging, 0.25% trypsin-EDTA (Thermo Fisher Scientific) was used as a dissociation reagent. The protocol for collection of human specimens was approved by the Institutional Review Board and informed consent was acquired from participants who provided specimens. Primary glioma cells were maintained as nonadhesive spheroids in flasks containing neurobasal medium (Thermo Fisher Scientific) supplemented with B27 Supplement Minus Vitamin A (Thermo Fisher Scientific), 100 μg/mL penicillin/streptomycin, GlutaMax (Thermo Fisher Scientific), and 50 μg/mL of both human EGF and FGF-2 (PeproTech). Spheres were dissociated using StemPro Accutase Cell Dissociation Reagent or TrypLE Express (Thermo Fisher Scientific).

HSV-1 viruses

We employed the HSVQuik method to engineer HSV-1 vectors as described previously (25, 26). First, the full-length *GADD34* gene was inserted into *Nco*I/*Hpa*I sites of a pTnestin-luc-b vector containing the nestin-hsp68 enhance- promoter element into pTransfer, by ligating the fragment obtained by enzymatic digestion of blunt-ended *Bst*XI/*Xho*I or *Hpa*I/*Xho*I of a pOTB7-GADD34 (NIH mammalian gene collection), respectively. These shuttle vectors were used to transform *E. coli* carrying the bacterial artificial chromosome (BAC) called fHsvQuik2, which has two flp recombination FRT sites within its UL39 locus but lacks the *EGFP* gene from fHsvQuik1 (26). FLP-FRT–mediated site-specific recombination between the shuttle vectors and fHsvQuik2 BAC results in fHsvQ2-nestin-GADD34 BAC vector. Vero cells were transfected with these BACs and a pc-nCre Cre recombinase-expression vector, to remove all the prokaryotic sequences portion from the shuttle vector flanking loxP sites. The resultant HSV-1 recombinant virus NG34 was generated and packaged in these cells. Other HSV-1 viruses and viral stocks were prepared as described previously (8, 27). NG34-gCRliFluc and rHSVQ-gCRli-Fluc oHSV are based on the fHSVQuik1 ($EGFP^+$) backbone and bear the gC late gene promoter driving expression of Rli-Fluc gene transcripts in the empty shuttle vector with and without a fragment of the hsp68-nestin promoter-enhancer–driven *GADD34* gene transcript unit, respectively (28).

Engineered cell lines

To obtain a lentivirus-based plasmid DNA encoding the *GADD34* gene, a fragment encoding full-length *GADD34* gene in pCR4blunt-TOPO (Thermo Fisher Scientific) were reinserted in the pLenti-CMVTRE3G puro DEST (w811–1; Addgene) vector using a site-specific recombination technique with a Gateway Cloning Kit (Thermo Fisher Scientific). The lentivirus-mediated transformation was performed using rtTA3G-expressing U251 (29) and selected using blasticidin S and puromycin, and clonal cells were analyzed by immunoblots against GADD34 as described below, after doxycycline (200 ng/mL) treatment for 24 hours. U87ΔEGFR-RliFluc cell line was generated from U87ΔEGFR as follows; a fragment encoding *RliFluc* cDNA (codon-optimized and red-shifted Luciola italica luciferase gene) was isolated by *Nhe*I/*Xho*I enzymatic digestion of pCSCW-RliFluc-

ImCherry (a gift from Bakhos A. Tannous, Massachusetts General Hospital, Boston, MA; ref. 30), and ligated into the unique *Sal*I site of pLenti PGK Puro DEST (w529–2; Addgene) after blunt-end treatment. The resulting lentivirus was used to infect U87ΔEGFR, and RliFluc-expressing cells were selected with puromycin. The human Nectin1-expressing lentivirus vector was generated as following; pcDNA3.1/zeo encoding full-length cDNA cut at an *Eco*RV site was constructed with the blunt-ended DNA fragment excised from the pCR4-PVRL1 (GenBank Accession: BC104948; Dana-Farber Cancer Institute, Boston, MA) by digestion with *Pme*I and *Not*I enzymes, followed by the reinsertion of *Pme*I-digested fragment at *Sal*I sites that were blunt-ended in pLenti PGK Hygro DEST (w530–1; Addgene). GL261 cells were infected with the lentivirus, and its derivative clone 4, designated as GL261N4, was selected and maintained in the presence of hygromycin (200 μg/mL), and confirmed by flow cytometry analysis (LSR II; BD Biosciences, CCVR Flow Cytometry Core in Beth Israel Deaconess Medical Center, Boston, MA) using anti-human CD111/Nectin-1 antibody (clone. R1.302; Biolegend).

Cell viability assay

Serially diluted aliquots of oHSV were prepared in a 96-well plate, and then single-cell suspension at the density of 20,000 cells per well was transferred to the new plates. After five-day incubation, the amount of ATPs was quantified using a CellTiter-Glo 2.0 Assay kit (Promega) and luminescent signals were read at 520 nm using a plate reader (POLARstar Omega; BMG Labtech). Data were normalized at maximum γ-axis values, followed by nonlinear regression analysis to plot the dose–response curves using Prizm 6 (GraphPad Software, Inc).

Western blot analyses

Cell lysates were prepared in lysis buffer, consisting of 50 mmol/L Tris-Cl (pH 7.4), 150 mmol/L NaCl, 2.5 mmol/L EDTA, 0.5 % Triton X-100, 40 μmol/L MG132, 5 mmol/L DTT, PhosSTOP (Sigma) and protease inhibitor cocktail (Roche), sonicated before centrifugation at 20,000 × *g* for 10 minutes at 4°C. Supernatants were used for immunoblot analyses using antibodies against GADD34 (Santa Cruz Biotechnology), eIF2α, phosphor-eIF2α at serine-51 (Cell Signaling Technology), HSV-1 ICP4 (Virusys), αTubulin (Sigma), and γTubulin (Sigma).

Animal use

All experimental procedures using animals were carried out under an animal protocol reviewed and approved by the Harvard Center for Comparative Medicine (HCCM) and BWH's IACUCs, and performed in accordance with relevant guidelines and regulations. Female gender-matched tumors and mice were utilized for the *in vivo* studies. Six- to 8-week-old athymic nude and BALB/c mice were purchased from Envigo. For the *in vivo* oHSV therapeutic study, dissociated U87ΔEGRF-RliFluc or G35 tumor cells (100,000 cells in 5 μL of HBSS or D-PBS buffer) were injected intracerebrally at stereotactic coordinates (ventral 3.5-mm, rostral 0.5-mm and right lateral 2.0-mm from the bregma using a stereotaxic apparatus (David Korp Instruments) to establish the xenograft tumor in the brains of athymic nude mice, followed by the intratumoral injection of oHSV at indicated timing and doses described in Fig. 4 and Supplementary Fig. S5. For the toxicity study, purified

viruses were directly injected intracerebrally at the indicated doses described in Fig. 5. For *in vivo* bioluminescent imaging in a U87ΔEGRF-RliFluc xenograft model, D-luciferin (Promega; dissolved in sterile D-PBS) at a dose of 3 mg per 20-g body weight was intraperitoneally injected in mice under an anesthetic condition with isoflurane vaporizer. Light-emitted imaging was acquired by IVIS Lumina LT with Living Image software (Perkin-Elmer) every 60 seconds, and images with peak signals were selected for the figures. Kaplan–Meier analysis with log-rank test or Gehan–Breslow–Wilcoxon test were performed using Prism 6 software.

IHC analysis

Brain tissues were fixed with 10% neutralization buffer and embedded in paraffin in the BWH pathology core facility (Boston, MA). The sectioned samples slides were deparaffinized and rehydrated using xylene and subsequently ethanol. Antigens were retrieved by boiling in citrate buffer, after treating with 2% normal goat serum/TBS, and then 0.3% hydrogen peroxide in methanol. Primay antibodies we used are follows: anti-HSV1/2 (Dako, B0114), anti-mouse CD45 (BD Biosciences, 553076), anti-NeuN (Abcam, ab177487), anti-Iba1 (Abcam, ab178846), and antimouse GFAP (Dako, Z0334). After staining with secondary antibodies of HRP-polymer IgG (Abcam) against rabbit (ab214880, Abcam) or rat (ab214882, Abcam), Metal Enhanced DAB Substrate Kit (34065, Thermo Fisher Scientific) was used for detection. All sections were counterstained with hematoxylin. Nikon Ti microscopy system was used to capture images.

Results

Glioma cells induced to express GADD34 significantly enhance the replication of an ICP34.5–mutant oHSV

We first aimed to test whether GADD34 by itself could affect the infection of an HSV1 that is mutated in ICP34.5. We engineered human U251 glioma cells to express a full-length GADD34 in response to doxycycline induction. The reason for employing a doxycycline-inducible system was due to the poor growth of stable GADD34 transfectants (data not shown), probably because the dominant PP1–GADD34 interaction itself has affected other PP1-interacting proteins (31). Upon doxycycline withdrawal, GADD34 was quickly degraded, which was reversed by MG-132 treatment (Fig. 1A). Next, we infected doxycycline-treated U251 cells with an ICP34.5-null HSV-1 (31). There was at least a log increase in yield of this ICP34.5-null HSV-1 when GADD34 was induced compared with the doxycycline-treated control cells without GADD34 induction (Fig. 1B). These results implied that expression of GADD34 could increase the yield of an ICP34.5-null HSV1 in human glioma cells.

NG34, a novel oHSV, where GADD34 expression is under control of the nestin promoter/enhancer, exhibits replicative kinetics similar to rQNestin34.5

On the basis of these results, we engineered a new oHSV with the rQNestin34.5 backbone, NG34. This novel oHSV possesses a nestin enhancer-*hsp68* promoter to drive expression of GADD34 in the HSV *Ul39* locus, encoding the viral ribonucleotide reductase, ICP6. Lack of ICP6 restricts oHSV's replicative selectivity to mitotic cells or cells with p16 tumor

suppressor defects. NG34 also possesses diploid deletion of the endogenous $\gamma_1$34.5 genes (Fig. 2A). NG34 should thus be genetically very similar to rQNestin34.5, currently in phase I clinical trials for recurrent GBM (8, 26). Both ICP34.5 and GADD34 are known to reverse suppression of global protein translation through dephosphorylation of eIF2α. To validate the functionality of the virally expressed *GADD34* gene, we analyzed the phosphorylation status of eIF2α by Western blot analysis. As expected, phosphorylated eIF2α was not detected in U251 glioma cells infected with parental wild-type F strain, rQNestin34.5, or NG34, while eIF2α was phosphorylated in cells infected with ICP34.5-null oHSV (rHSVQ; Fig. 2B). This result confirmed that GADD34 functions like ICP34.5 in inhibiting the phosphorylation of eIF2α and blocking translation, an innate host defense mechanism against viral infection. To further validate the functionality of GADD34, we performed single step-growth curve assays. Figure 2C shows that the replicative kinetics of NG34 were like those of rQNestin34.5. As expected, yields of the ICP34.5-null oHSV (rHSVQ) were 1 to 2 logs less at most of postinfection time points. Cytotoxicity in cultured astrocytes was also similar for both oHSVs (Supplementary Fig. S1). These results thus further confirmed that GADD34 functionally improved the replicative kinetics of an ICP34.5-null oHSV, to a degree like that observed with rQNestin34.5.

NG34 cytotoxicity and replication in a panel of patient-derived glioma cells are like those of rQNestin34.5 and higher than those of rHSVQ1, an ICP34.5-defective oHSV

We further validated the oncolytic capacity of NG34 against seven different human patient-derived GBMs, grown as short-term neurosphere cultures. Each was infected with each oHSV at various MOIs. Figure 3 shows that the dose-effect curves for the two oHSVs (NG34 and rQNestin34.5) were similar, although NG34 was more cytotoxic for some GBMs (G9, G30, G35). NG34 did not grow as well against human U2OS osteosarcoma cells, which do not express nestin, while NG34 cytotoxicity against GBM cells was higher than that of the ICP34.5-null oHSV, rHSVQ (Table 1; Supplementary Figs. S2). In agreement with our previous study (8), replication of NG34 and rHSVQ was marginal in cultured astrocytes and cytotoxicities were less than that seen in GBMs (Supplementary Figs. S1 and S2). We further analyzed the efficacy of viral replicative kinetics by assaying the expression of late genes encoding structural proteins (e.g., envelope and tegument proteins). This experiment was performed by engineering NG34 and rHSVQ to express the luciferase gene under the control of the HSV glycoprotein C (*gC*) late gene promoter that is only expressed during viral replications. Human U251, G9Rluc, and G87Rluc glioma cells were then infected with these expressing luciferase oHSVs. NG34 expressed luciferase approximately three times higher than rHSVQ at 15 hours postinfection (p.i.) (Supplementary Fig. S3). Overall, these results showed that NG34 replication was more extensive and its cytotoxicity was more potent than an ICP34-null oHSV in several GBM cells.

In vivo efficacy studies

We then compared the therapeutic efficacy of NG34 and rQNestin34.5 in intracranial human GBM xenograft mouse models. To monitor tumor growth using bioluminescence imaging (BLI), we first engineered human U87ΔEGFR-RliFluc cells, in which the red-shifted *Luciola Italica* luciferase (Rli-Fluc) gene is constitutively expressed (30). At seven days post-tumor implantation into the brains of athymic nude mice, the emission light intensity in

brains from D-luciferin–injected mice was measured to allocate U87ΔEGFR-RliFluc bearing mice into three groups with almost identical signal intensity before starting treatment with NG34, rQNestin34.5, or HBSS vehicle (Supplementary Fig. S4). To minimize artifacts related to different tumor size affecting therapeutic outcomes, two mice with the lowest BLI signal were placed in the HBSS vehicle control group. It should be noted though that these mice did eventually develop tumors during the second week (Supplementary Fig. S4) and had to be euthanized due to deteriorating health. Intratumoral administration of NG34, rQNestin34.5, or vehicle control led to a reduction in signal intensity for four of five mice in the NG34 and rQNestin34.5 groups compared with zero of five in control groups (Supplementary Fig. S4). This also led to a significant survival extension for the NG34 and rQNestin34 groups compared with the HBSS control group (Fig. 4A; Supplementary Fig. S5). With 80% power and Type I error probability of 0.05, the maximum detectable relative risk was 0.74 for the NG34 (or rQNestin34.5) group compared with the control group in a two-sided test. Thus, with an observed effect size of 0.1, there is sufficient power to detect a difference between the treatment group and the control group. An *in vivo* experiment using a second human xenograft model was also performed by using neurosphere cultured human gliomas. Human G35 gliomas are fairly aggressive, and mice in the control group reached humane endpoints within 10–15 days of tumor implantation (Fig. 4B). Both NG34 and rQNestin34.5 still led to statistically significant improvements in mouse survival (Fig. 4B) even in this aggressive GBM model. The sum of these findings shows that NG34 was as potent in its therapeutic efficacy as rQnestin34.5 against human GBM xenograft models.

We also performed the therapeutic evaluation of NG34 in immunocompetent C57Bl/6 strain mice bearing GL261 murine glioma. We found that GL261 is resistant to HSV-1 infection, but that introduction of one of the HSV-1 entry receptors (Nectin-1/PVRL1/CD111; refs. 32, 33) in GL261 cells restores their susceptibility to HSV-1 (data not shown). Thus, we engineered human Nectin-1–expressing GL261 glioma cells (GL261N4) that overexpress Nectin-1 (Fig. 4C). At 7 days postimplantation of GL261N4 in immunocompetent mouse brains, NG34 or vehicle control were intratumorally injected. NG34 led to a significant extension of survival when compared with vehicle-treated mice (Fig. 4D). Therefore, both human xenografts and immunocompetent models of human GBMs were responsive to NG34 administration.

NG34 is less neurotoxic than rQNestin34.5

Finally, we asked whether NG34 was less neurovirulent than rQNestin34.5. An intracerebral *in vivo* challenge experiment was performed with a high dose of these oHSVs (3×10^6 pfu) in the brains of BALB/c mice, known to be sensitive to HSV-1 infection. After 70 days, NG34 demonstrated significantly better tolerability (one lethality out of six), when compared with rQNestin34.5 (five lethalities out of six; Fig. 5A). The body weight of surviving mice showed a continuous increase over the 70-day period in the both groups (Fig. 5B). The same experiment was also performed in athymic mice in three escalating doses. While neither oHSV was lethal at a dose of 3×10^4 pfu in athymic mice, both oHSV at the dose of 3×10^6 pfu led to 100% lethality (Fig. 5C). Again, NG34 appeared to be better tolerated compared with rQNestin34.5 when injected intracerebrally at 3×10^5 pfu (Fig. 5C). The body weight of these surviving mice also increased over the 70-day period of the

experiment (Fig. 5D). In fact, for most mice that suffered from neurotoxicity, there was fairly rapid loss of body weight. If they were able to fight off the neurotoxic event, they were able to rapidly regain body weight. Because NG34 appeared to be more toxic in athymic nude mice compared with immunocompetent BALB/c mice despite the lower intracerebral dose, we compared the transcription profiles of type I IFNs, TNFα, IL1β, IL27, and IL6 between these two mouse strains, four days after brain inoculation with NG34 at a dose of 3×10^5 pfus. Supplementary Figure S6 shows that the most significant change was an elevation in IL6 and IL27 in BALB/c versus athymic mice treated with NG34, while elevations of the other tested cytokines was fairly similar between athymic and BALB/c mice. Histopathologic analysis of the brains of athymic mice that exhibited signs of neurotoxicity at day 3 (3×10^6 pfu) or day 5 (3×10^5 pfu) after infection showed broad areas of HSV-1 antigenicity (Fig. 6A and C), along the needle injection tract (Fig. 6A). There was colocalization of positive HSV antigenicity with neuron ($NeuN^+$) and glia ($GFAP^+$) antigenicity in cerebral cortex (Supplementary Fig. S7). We observed different level of recruitment of innate immune cells in analyzed brains (Fig. 6E–L). Parenchymal infiltrates of $CD45^+$ immune cells and $Iba1^+$ microglia–positive areas were more prominent at the lower dose of NG34 (Fig. 6F and J), whereas $CD45^+$ cell infiltrates were less apparent for either oHSV at 3×10^6 pfu (Fig. 6E and G). Accumulation of $Iba1^+$ microglia within the anti-$HSV\text{-}1^+$ brain region and hemisphere was not apparent with rQNestin34.5 (Fig. 6K). Taken together, these studies showed that NG34 appeared to have an improved neurotoxicity profile when compared with rQNestin34.5. It also suggested that the degree of innate immune cell infiltration in $HSV\text{-}1^+$ regions may vary based on dose.

Discussion

Oncolytic virus (OV) therapy has now become a clinical reality with regulatory approval of the first product for melanoma (i.e., Imlygic, T-VEC, also known as OncoVEX-GM-CSF; ref. 34) and several other OVs being in advanced phases of clinical trials (35). For other cancers, such as GBM, OVs should also provide promising results. All clinical trials of oHSVs up-to-date have utilized constructs where the viral *ICP34.5* gene is deleted or defective in some form to minimize neurovirulence to normal brain. However, the lack of ICP34.5 also significantly attenuates the capacity of the oHSV to sustain robust replication in infected GBM cells. To overcome this obstacle, we have engineered and preclinically tested rQNestin34.5 (8), an oHSV where one copy of the viral *ICP34.5* gene is reinserted under control of the cellular nestin promoter, as nestin is highly expressed in GBM in adult human brain (36–39). A phase I clinical trial of this agent against recurrent GBM is currently actively accruing patients and is supported by an FDA-approved IND. However, spurious expression of ICP34.5 still carries a theoretical risk of neurotoxicity. We thus reasoned that the human *GADD34* gene, a mammalian ortholog of HSV ICP34.5, could be a substitute that might enable the same level of viral replication in infected GBM cells as wild-type ICP34.5-positive oHSV, yet still display the reduced neurotoxicity of ICP34.5-negative oHSV. Here we show that (i) newly engineered oHSV NG34 replicates in GBM cells *in vitro* with similar kinetics as those exhibited by rQNestin34.5; (ii) the dose response of NG34 toxicity shown in GBM cells is equivalent to, or in some cases even better when compared with rQNestin34.5; (iii) the *in vivo* antitumor efficacy of NG34 in two human

orthotopic GBM models in athymic mice is similar to that of rQNestin34.5; (iv) NG34 also shows significant antitumor efficacy in a syngeneic mouse GBM model; and (v) intracerebral injection of NG34 in brains of immunocompetent and athymic mice shows significantly better tolerability when compared with rQNestin34.5. Taken together, these results demonstrate that, NG34 and rQNestin34.5 possess similar antitumor efficacy against GBM models, but NG34 appears to be less toxic when injected into mice brains without tumor.

As previously reported by others (18–20), we confirmed that GADD34 expression prevents phosphorylation of eIF2α at the serine-51 residue after infection with a $\gamma_1$34.5-null HSV (Fig. 2B). The translation initiation factor eIF2α is one subunit of the ternary EIF2 complex, whose formation is modulated by the phosphorylation of eIF2α (40). The eIF2 complex is primarily responsible for the binding of the initiator methionyl-tRNA to the 40S ribosomal subunit and catalyzes the initiation of protein synthesis (18). In response to HSV-1 infection, cells (including GBM cells) immediately activate PKR-mediated phosphorylation of eIF2α and suppress viral protein synthesis. HSV-1 ICP34.5 counteracts this process by dephosphorylating eIF2α through its binding to and transport of the PP1 phosphatase to eIF2 within the HSV-1–infected cell (12, 17). The carboxyl-terminal PP1 binding domain of mammalian GADD34 and viral ICP34.5 are both conserved as PP1-interacting proteins that lead to the dephosphorylation of eIF2α via the activity of PP1 (13). It has been reported that upregulation of cellular GADD34 can enhance the activity of oHSV-1 in glioma in the context of stress responses, such as treatment with temozolomide or culture under hypoxic conditions (41, 42). In addition to the NG34 approach we describe here, others have also engineered oHSV to modify or duplicate ICP34.5 function to enhance oHSV replication in tumors while minimizing ICP34.5 neurotoxicity. A study by Rabkin and colleagues demonstrated that Δ68H(–6) virus, an oHSV where the Beclin1-binding domain of the *$\gamma_1$34.5* gene was deleted, was highly neuroattenuated compared with HSV-1 that expresses wild-type ICP34.5 in A/J mice (10). On the basis of the finding that the HSV1 Us11 also suppresses phosphorylation of eIF2α (11, 17), Todo and colleagues engineered a $\gamma_1$34.5-null G47Δ oHSV encoding a *Us11* gene under transcriptional control of the immediate-early *Us12* promoter (43) and this oHSV (G47Δ) is being tested in clinical trials for GBM patients in Japan (44). In another approach, the TRS1 and IRS1 gene products (C130 and C134, respectively) of human cytomegalovirus have been engineered into an ICP34.5-null oHSV, as they have been shown to substitute for ICP34.5 function (45).

Wild-type HSV-1 neurotoxicity during the viral lytic cycle has been extensively studied (46, 47). Intracerebral inoculation of GADD34-encoding NG34 reduced mouse lethality when compared with injection of the ICP34.5-encoding rQNestin34.5, but did not eliminate neurotoxicity completely. It is interesting to speculate on why a human protein such as GADD34 would still show some extent of neurotoxicity when expressed from an oHSV. To provide possible explanations for this finding, we should consider two general topics: the first relates to the spurious expression of GADD34 or ICP34.5 in normal neural cells, while the second relates to the direct involvement of GADD34 in neurotoxicity. In regard to the first topic, the Nestin promoter/enhancer transcriptional element drives expression of GADD34 in NG34 and ICP34.5 in rQNestin34.5. The Nestin enhancer should be transcriptionally active only in GBM cells and inactive in normal neural cells.Acouple of

explanations could be entertained (i) there is low-level expression of nestin in normal brain cells, that produces sufficient amount of GADD34 or ICP34.5 for progeny production leading to neurotoxicity, and/or (ii) there is transcriptional leakage of *GADD34* or *ICP34.5* gene controlled under the hybrid Nestin/Hsp68 promoter and gene regulatory elements in NG34 or rQNestin34.5 that leads to their protein production. We believe that the first explanation is more likely based on the data we have in hand. For the rQNestin34.5 IND application, we performed extensive studies related to nestin expression in mouse brains as well as in adult human brains. We have found that the brains of young adult mice do express enough nestin that can be detected by IHC, particularly in tanycytes around the ependymal layers of the ventricle (data not shown). However, brains of human adults do not exhibit expression of nestin detectable by IHC, either in brain tissues surrounding a GBM, or brains after radiation or chemotherapy, and brain areas around ventricles (data not shown). There have also been several reports to show that nestin is not expressed in adult human brains or, if it is, it is discreetly located in sparse areas of deep brain nuclei (36–39). These human studies would bring concern that data obtained from mice may overestimate the neurotoxicity of oHSVs where nestin transcriptional elements are driving expression of viral genes associated with neurovirulence. The second explanation is less likely, that the *hsp68* gene promoter without enhancer elements does possess some transcriptional leakage (data not shown). However, we did not observe progeny virions in primary tissue culture cells such as astrocytes and smooth muscle cells (data not shown). Compared to GADD34-null and ICP34.5-null rHSVQ virus, cytotoxicity of NG34 was not significant in non-nestin–expressing U2OS cells. Thus, we believe that the transcriptional leakage explanation is possible but not likely to contribute to *in vivo* neurotoxicity.

The ICP34.5$^+$ rQNestin34.5 oHSV exhibited higher neurotoxicity than the GADD34$^+$ NG34. Orvedahi and colleagues showed that inhibiting neuronal autophagy by ICP34.5 leads to fatal HSV-1 encephalitis in mice (48). Autophagy is especially important for nondividing neuronal tissue to maintain cellular homeostasis and protein's quality control, as well as to prevent neurodegeneration. Inhibition of the autophagy flux has been shown to be detrimental to neuronal protection after traumatic brain injury, which would promote neurodegenerative disorders. Interestingly, GADD34 expression during periods of cellular stress may promote autophagy (21–23). In addition to the high binding affinity of ICP34.5 to Beclin-1 (GADD34 does not bind to Beclin-1), ICP34.5 also regulates the IFN-I pathway via an interaction between the cellular TANK binding kinase I (TBK1) and the amino-terminus of ICP34.5 (49, 50). IFN-I signal the cascade of antiviral innate immune responses that modulate viral replication. Hence ICP34.5 may also facilitate neurovirulence through the regulation of IFN-I response in mice, a function that GADD34 is not known to possess (51). This could thus provide an additional explanation of why ICP34.5 may be more neurotoxic than GADD34. Finally, ICP34.5 also provides structural functions as part of the tegument compartment of viral particles (52). The ICP34.5 protein in rQNestin34.5 thus enters into cells, such as neuron and astrocytes, which may be nonpermissive for replication but still infection-susceptible: this by itself, can be neurotoxic even in the absence of active viral gene expression. Instead, GADD34 is not a structural component of the HSV-1 virion, and thus would not be transmitted in the absence of active gene expression. This may help to limit anti-HSV T-cell immunity mediated through autophagy in cells with primary infection

with an ICP34.5$^+$ virus (53). The quick turn-over of GADD34 protein also would limit its toxicity (54). It should be also noted that the neurotoxicity of GADD34 may also depend on HSV strains and the context of experimental settings. In an experimental mouse stroke model, McCabe and colleagues reported that GADD34 restores virulence of the $\gamma_1$34.5-null HSV1716 virus, constructed from HSV17$^+$ strain, which is highly neurovirulent compared with the F strain used as backbone for our oHSVs (55, 56). The intracerebral inoculation experiment also demonstrated that immunocompetent BALB/c mice tolerated NG34 more than athymic mice. Except for a difference in increased IL6 and IL27 elevation, both mice responded to NG34 with similar elevation of other tested cytokines. Mice with intact immune systems are more likely to resist NG34 infection better than immunodeficient mice. The role of the differential IL6 and IL27 elevation can also be an interesting topic for discussion. Published studies report that IL6, as an acute phase reactant, promotes humoral immunity and lineage commitment in the Th17 subset of helper T cells, which athymic mice lack (57, 58). Beyond adaptive immunity, IL6 can also contribute to restrict HSV-1 neurotoxicity. Microglia produce IL6 upon HSV-1 infection to prevent neuronal loss during acute infection with HSV-1 (59). Our data seems to show that acute infection with high doses of rQNestin34.5 did not have as much Iba-positive microglia as observed at low-dose infection, suggesting that microglia are an important player in the survival from acute infection and protection from neuronal loss. It is also reported that IL6 is regulated via the GADD34–PP1 pathway but it is not clear whether NG34-expressing GADD34 contribute to this IL6 pathway (60). We also found a surge of IL27 expression upon NG34 infection. IL27 is a member of the IL6 cytokine family and may regulate antiviral T-cell immunity at the acute phase and contribute to protection in BALB/c mice (61). Since IL27 is produced by microglia and macrophages in the CNS upon viral infection (62) and we observed enrichment of microglia and CD45$^+$ cells within HSV-1–positive brain area, IL27 may mark the immune response of innate immune cells upon HSV-1 infection. The upregulation of IL1β, IFNβ, and TNFα instead may derive from innate immune cells present in both athymic and immunocompetent mice and contribute to the transition from innate to adaptive immunity (63). In addition, GADD34 expressed by NG34 can promote PP1-mediated dephosphorylation of TSC1, I-kB kinase (IKK), and TGFβ receptor 1 (TGFβR1; refs. 19, 21, 22, 31, 64, 65). The persistent PP1 interaction of GADD34 may also disturb the functionality of other PP1-interacting protein complexes, as PP1 is a major phosphoprotein phosphatase of protein Ser/Thr phosphatases, and forms as many as 650 distinct complexes (31).

Despite the reduced neurotoxicity of NG34 compared with rQNestin34.5, there was still evidence of positive HSV antigenicity in normal brain cells upon inoculation. IHC appeared to show that this antigenicity occurred in cells that were neurons or astrocytes. Interestingly, we know that the trauma from needle injection seems to upregulate nestin-positive reactive glia in mice and that there are a considerable number of nestin-positive neurons in the brain of mice, including the subpendymal zone and along the walls of the third ventricle (data not shown). This nestin positivity in mice brains will thus allow for probable replication of the engineered oHSVs used in our study in mice.

In summary, we show that a novel oncolytic HSV-1 encoding *GADD34*, NG34, can provide an alternative to expression of ICP34.5 to enhance viral replication and minimize

neurotoxicity. Although there have not been neurotoxicities to date with oHSVs in clinical trials, all current oHSVs lack ICP34.5 function. rQNestin34.5 is the first ICP34.5-positive oHSV to be injected in humans with cancer under a current IND. Although it is not known whether a neurotoxic MTD will be encountered with this particular oHSV, finding one would not be unexpected. In this context, NG34 may represent a possible solution for such an eventuality. Additional preclinical testing in animal models may thus be warranted to justify its use in clinical practices via an IND.

Supplementary Material

Refer to Web version on PubMed Central for supplementary material.

Acknowledgments

This work were supported by NIH 2P01CA163205 (to E.A. Chiocca) and American Brain Tumor Association (to C. Passaro, Basic Research Fellowship).

References

1. Ostrom QT, Gittleman H, Xu J, Kromer C, Wolinsky Y, Kruchko C, et al. CBTRUS statistical report: primary brain and other central nervous system tumors diagnosed in the United States in 2009–2013. Neuro Oncol 2016;18:v1–v75. [PubMed: 28475809]
2. Brennan CW, Verhaak RG, McKenna A, Campos B, Noushmehr H, Salama SR, et al. The somatic genomic landscape of glioblastoma. Cell 2013;155:462–77. [PubMed: 24120142]
3. Patel AP, Tirosh I, Trombetta JJ, Shalek AK, Gillespie SM, Wakimoto H, et al. Single-cell RNA-seq highlights intratumoral heterogeneity in primary glioblastoma. Science 2014;344:1396–401. [PubMed: 24925914]
4. Reardon DA, Freeman G, Wu C, Chiocca EA, Wucherpfennig KW, Wen PY, et al. Immunotherapy advances for glioblastoma. Neuro Oncol 2014;16: 1441–58. [PubMed: 25190673]
5. Tivnan A, Heilinger T, Lavelle EC, Prehn JH. Advances in immunotherapy for the treatment of glioblastoma. J Neuro Oncol 2016.
6. New drug and biological drug products; evidence needed to demonstrate effectiveness of new drugs when human efficacy studies are not ethical or feasible. Final rule. Federal Register 2002;67:37988–98. [PubMed: 12049094]
7. Ning J, Wakimoto H. Oncolytic herpes simplex virus-based strategies: toward a breakthrough in glioblastoma therapy. Front Microbiol 2014; 5:303. [PubMed: 24999342]
8. Kambara H, Okano H, Chiocca EA, Saeki Y. An oncolytic HSV-1 mutant expressing ICP34.5 under control of a nestin promoter increases survival of animals even when symptomatic from a brain tumor. Cancer Res 2005;65: 2832–9. [PubMed: 15805284]
9. Kaufmann JK, Chiocca EA. Glioma virus therapies between bench and bedside. Neuro Oncol 2014;16:334–51. [PubMed: 24470549]
10. Kanai R, Zaupa C, Sgubin D, Antoszczyk SJ, Martuza RL, Wakimoto H, et al. Effect of gamma34.5 deletions on oncolytic herpes simplex virus activity in brain tumors. J Virol 2012;86:4420–31. [PubMed: 22345479]
11. He B, Chou J, Brandimarti R, Mohr I, Gluzman Y, Roizman B. Suppression of the phenotype of gamma(1)34.5- herpes simplex virus 1: failure of activated RNA-dependent protein kinase to shut off protein synthesis is associated with a deletion in the domain of the alpha47 gene. J Virol 1997;71:6049–54. [PubMed: 9223497]
12. Li Y, Zhang C, Chen X, Yu J, Wang Y, Yang Y, et al. ICP34.5 protein of herpes simplex virus facilitates the initiation of protein translation by bridging eukaryotic initiation factor 2alpha (eIF2alpha) and protein phosphatase 1. J Biol Chem 2011;286:24785–92. [PubMed: 21622569]

13. Zhang C, Tang J, Xie J, Zhang H, Li Y, Zhang J, et al. A conserved domain of herpes simplex virus ICP34.5 regulates protein phosphatase complex in mammalian cells. FEBS Lett 2008;582:171–6. [PubMed: 18068675]
14. Wu DY, Tkachuck DC, Roberson RS, Schubach WH. The human SNF5/INI1 protein facilitates the function of the growth arrest and DNA damage-inducible protein (GADD34) and modulates GADD34-bound protein phosphatase-1 activity. J Biol Chem 2002;277:27706–15. [PubMed: 12016208]
15. Connor JH, Weiser DC, Li S, Hallenbeck JM, Shenolikar S. Growth arrest and DNA damage-inducible protein GADD34 assembles a novel signaling complex containing protein phosphatase 1 and inhibitor 1. Mol Cell Biol 2001;21:6841–50. [PubMed: 11564868]
16. He B, Gross M, Roizman B. The gamma134.5 protein of herpes simplex virus 1 has the structural and functional attributes of a protein phosphatase 1 regulatory subunit and is present in a high molecular weight complex with the enzyme in infected cells. J Biol Chem 1998;273: 20737–43. [PubMed: 9694816]
17. Mulvey M, Poppers J, Sternberg D, Mohr I. Regulation of eIF2alpha phosphorylation by different functions that act during discrete phases in the herpes simplex virus type 1 life cycle. J Virol 2003;77:10917–28. [PubMed: 14512542]
18. Rojas M, Vasconcelos G, Dever TE. An eIF2alpha-binding motif in protein phosphatase 1 subunit GADD34 and its viral orthologs is required to promote dephosphorylation of eIF2alpha. Proc Natl Acad Sci U S A 2015;112:E3466–75. [PubMed: 26100893]
19. Moreno JA, Radford H, Peretti D, Steinert JR, Verity N, Martin MG, et al. Sustained translational repression by eIF2alpha-P mediates prion neurodegeneration. Nature 2012;485:507–11. [PubMed: 22622579]
20. Choy MS, Yusoff P, Lee IC, Newton JC, Goh CW, Page R, et al. Structural and functional analysis of the GADD34:PP1 eIF2alpha phosphatase. Cell Rep 2015;11:1885–91. [PubMed: 26095357]
21. Hyrskyluoto A, Reijonen S, Kivinen J, Lindholm D, Korhonen L. GADD34 mediates cytoprotective autophagy in mutant huntingtin expressing cells via the mTOR pathway. Exp Cell Res 2012;318:33–42. [PubMed: 21925170]
22. Uddin MN, Ito S, Nishio N, Suganya T, Isobe K. GADD34 induces autophagy through the suppression of the mTOR pathway during starvation. Biochem Biophys Res Commun 2011;407:692–8. [PubMed: 21439266]
23. Ito S,Tanaka Y, Oshino R, Aiba K, Thanasegaran S, Nishio N, et al. GADD34 inhibits activation-induced apoptosis of macrophages through enhancement of autophagy. Sci Rep 2015;5:8327. [PubMed: 25659802]
24. Ausman JI, Shapiro WR, Rall DP. Studies on the chemotherapy of experimental brain tumors: development of an experimental model. Cancer Res 1970;30:2394–400. [PubMed: 5475483]
25. Terada K, Wakimoto H, Tyminski E, Chiocca EA, Saeki Y. Development of a rapid method to generate multiple oncolytic HSV vectors and their in vivo evaluation using syngeneic mouse tumor models. Gene Ther 2006;13: 705–14. [PubMed: 16421599]
26. Nakashima H, Chiocca EA. Modification of HSV-1 to an oncolytic virus. Methods Mol Biol 2014;1144:117–27. [PubMed: 24671680]
27. Nakashima H, Kaufmann JK, Wang PY, Nguyen T, Speranza MC, Kasai K, et al. Histone deacetylase 6 inhibition enhances oncolytic viral replication in glioma. J Clin Invest 2015;125:4269–80. [PubMed: 26524593]
28. Yamamoto S, Deckter LA, Kasai K, Chiocca EA, Saeki Y. Imaging immediate-early and strict-late promoter activity during oncolytic herpes simplex virus type 1 infection and replication in tumors. Gene Ther 2006;13:1731–6. [PubMed: 16871231]
29. Nakashima H, Nguyen T, Goins WF, Chiocca EA. Interferon-stimulated gene 15 (ISG15) and ISG15-linked proteins can associate with members of the selective autophagic process, histone deacetylase 6 (HDAC6) and SQSTM1/p62. J Biol Chem 2015;290:1485–95. [PubMed: 25429107]
30. Maguire CA, van der Mijn JC, Degeling MH, Morse D, Tannous BA. Codonoptimized Luciola italica luciferase variants for mammalian gene expression in culture and in vivo. Mol Imag 2012;11:13–21.

31. Bollen M, Peti W, Ragusa MJ, Beullens M. The extended PP1 toolkit: designed to create specificity. Trends Biochem Sci 2010;35:450–8. [PubMed: 20399103]
32. Krummenacher C, Nicola AV, Whitbeck JC, Lou H, Hou W, Lambris JD, et al. Herpes simplex virus glycoprotein D can bind to poliovirus receptor-related protein 1 or herpesvirus entry mediator, two structurally unrelated mediators of virus entry. J Virol 1998;72:7064–74. [PubMed: 9696799]
33. Geraghty RJ, Krummenacher C, Cohen GH, Eisenberg RJ, Spear PG. Entry of alphaherpesviruses mediated by poliovirus receptor-related protein 1 and poliovirus receptor. Science 1998;280:1618–20. [PubMed: 9616127]
34. Andtbacka RH, Kaufman HL, Collichio F, Amatruda T, Senzer N, Chesney J, et al. Talimogene laherparepvec improves durable response rate in patients with advanced melanoma. J Clin Oncol 2015;33:2780–8. [PubMed: 26014293]
35. Pol J, Buque A, Aranda F, Bloy N, Cremer I, Eggermont A, et al. Trial Watch-Oncolytic viruses and cancer therapy. Oncoimmunology 2016;5: e1117740. [PubMed: 27057469]
36. Hendrickson ML, Rao AJ, Demerdash ON, Kalil RE. Expression of nestin by neural cells in the adult rat and human brain. PLoS One 2011;6: e18535. [PubMed: 21490921]
37. Sanai N, Tramontin AD, Quinones-Hinojosa A, Barbaro NM, Gupta N, Kunwar S, et al. Unique astrocyte ribbon in adult human brain contains neural stem cells but lacks chain migration. Nature 2004;427:740–4. [PubMed: 14973487]
38. Zhang M, Song T, Yang L, Chen R, Wu L, Yang Z, et al. Nestin and CD133: valuable stem cell-specific markers for determining clinical outcome of glioma patients. J Exp Clin Cancer Res 2008;27:85. [PubMed: 19108713]
39. Kitai R, Horita R, Sato K, Yoshida K, Arishima H, Higashino Y, et al. Nestin expression in astrocytic tumors delineates tumor infiltration. Brain Tumor Pathol 2010;27:17–21. [PubMed: 20425043]
40. Ernst H, Duncan RF, Hershey JW. Cloning and sequencing of complementary DNAs encoding the alpha-subunit of translational initiation factor eIF-2. Characterization of the protein and its messenger RNA. J Biol Chem 1987;262:1206–12. [PubMed: 2948954]
41. Aghi MK, Liu TC, Rabkin S, Martuza RL. Hypoxia enhances the replication of oncolytic herpes simplex virus. Mol Ther 2009;17:51–6. [PubMed: 18957963]
42. Aghi M, Rabkin S, Martuza RL. Effect of chemotherapy-induced DNA repair on oncolytic herpes simplex viral replication. J Nat Cancer Inst 2006;98: 38–50. [PubMed: 16391370]
43. Todo T, Martuza RL, Rabkin SD, Johnson PA. Oncolytic herpes simplex virus vector with enhanced MHC class I presentation and tumor cell killing. Proc Natl Acad Sci U S A 2001;98:6396–401. [PubMed: 11353831]
44. Fukuhara H, Ino Y, Todo T. Oncolytic virus therapy: A new era of cancer treatment at dawn. Cancer Sci 2016;107:1373–9. [PubMed: 27486853]
45. Shah AC, Parker JN, Gillespie GY, Lakeman FD, Meleth S, Markert JM, et al. Enhanced antiglioma activity of chimeric HCMV/HSV-1 oncolytic viruses. Gene Ther 2007;14:1045–54. [PubMed: 17429445]
46. Birmanns B, Reibstein I, Steiner I. Characterization of an in vivo reactivation model of herpes simplex virus from mice trigeminal ganglia. J Gen Virol 1993;74:2487–91. [PubMed: 8245867]
47. Halford WP, Balliet JW, Gebhardt BM. Re-evaluating natural resistance to herpes simplex virus type 1. J Virol 2004;78:10086–95. [PubMed: 15331741]
48. Orvedahl A, Alexander D, Talloczy Z, Sun Q, Wei Y, Zhang W, et al. HSV-1 ICP34.5 confers neurovirulence by targeting the Beclin 1 autophagy protein. Cell Host Microb 2007;1:23–35.
49. Ma Y, Jin H, Valyi-Nagy T, Cao Y, Yan Z, He B. Inhibition of TANK binding kinase 1 by herpes simplex virus 1 facilitates productive infection. J Virol 2012;86:2188–96. [PubMed: 22171259]
50. Verpooten D, Ma Y, Hou S, Yan Z, He B. Control of TANK-binding kinase 1-mediated signaling by the gamma(1)34.5 protein of herpes simplex virus 1. J Biol Chem 2009;284:1097–105. [PubMed: 19010780]
51. Davis KL, Korom M, Morrison LA. Herpes simplex virus 2 ICP34.5 confers neurovirulence by regulating the type I interferon response. Virology 2014; 468–470:330–9.

52. Radtke K, Kieneke D, Wolfstein A, Michael K, Steffen W, Scholz T, et al. Plus-and minus-end directed microtubule motors bind simultaneously to herpes simplex virus capsids using different inner tegument structures. PLoS Pathog 2010;6:e1000991. [PubMed: 20628567]

53. English L, Chemali M, Duron J, Rondeau C, Laplante A, Gingras D, et al. Autophagy enhances the presentation of endogenous viral antigens on MHC class I molecules during HSV-1 infection. Nat Immunol 2009;10: 480–7. [PubMed: 19305394]

54. Brush MH, Shenolikar S. Control of cellular GADD34 levels by the 26S proteasome. Mol Cell Biol 2008;28:6989–7000. [PubMed: 18794359]

55. McCabe C, White F, Brown SM, Macrae IM. GADD34 gene restores virulence in viral vector used in experimental stroke study. J Cereb Blood Flow Metab 2008;28:747–51. [PubMed: 17928799]

56. Sedarati F, Stevens JG. Biological basis for virulence of three strains of herpes simplex virus type 1. J Gen Virol 1987;68:2389–95. [PubMed: 2821178]

57. Acosta-Rodriguez EV, Napolitani G, Lanzavecchia A, Sallusto F. Interleukins 1beta and 6 but not transforming growth factor-beta are essential for the differentiation of interleukin 17-producing human T helper cells. Nat Immunol 2007;8:942–9. [PubMed: 17676045]

58. Kopf M, Baumann H, Freer G, Freudenberg M, Lamers M, Kishimoto T, et al. Impaired immune and acute-phase responses in interleukin-6-deficient mice. Nature 1994;368:339–42. [PubMed: 8127368]

59. Chucair-Elliott AJ, Conrady C, Zheng M, Kroll CM, Lane TE, Carr DJ. Microglia-induced IL-6 protects against neuronal loss following HSV-1 infection of neural progenitor cells. Glia 2014;62:1418–34. [PubMed: 24807365]

60. Clavarino G, Claudio N, Couderc T, Dalet A, Judith D, Camosseto V, et al. Induction of GADD34 is necessary for dsRNA-dependent interferon-beta production and participates in the control of Chikungunya virus infection. PLoS Pathog 2012;8:e1002708. [PubMed: 22615568]

61. Fabbi M, Carbotti G, Ferrini S. Dual roles of IL-27 in cancer biology and immunotherapy. Mediators Inflamm 2017;2017:3958069. [PubMed: 28255204]

62. Klein RS, Hunter CA. Protective and pathological immunity during central nervous system infections. Immunity 2017;46:891–909. [PubMed: 28636958]

63. Sergerie Y, Rivest S, Boivin G. Tumor necrosis factor-alpha and interleukin-1 beta play a critical role in the resistance against lethal herpes simplex virus encephalitis. J Infect Dis 2007;196:853–60. [PubMed: 17703415]

64. Heroes E, Lesage B, Gornemann J, Beullens M, Van Meervelt L, Bollen M. The PP1 binding code: a molecular-lego strategy that governs specificity. Febs J 2013;280:584–95. [PubMed: 22360570]

65. Watanabe R, Tambe Y, Inoue H, Isono T, Haneda M, Isobe K, et al. GADD34 inhibits mammalian target of rapamycin signaling via tuberous sclerosis complex and controls cell survival under bioenergetic stress. Int J Mol Med 2007;19:475–83. [PubMed: 17273797]

Translational Relevance

Glioblastoma represents a formidable unmet medical need. Recently, oncolytic viruses (OVs) have shown evidence of success against cancers such as melanoma and OVs are also being tested in clinical trials for glioblastoma. Here, we test the efficacy and toxicity of a novel oncolytic virus (NG34) based on herpes simplex virus type-1 (HSV-1) in preclinical mouse models of glioblastoma. This oncolytic HSV-1 (oHSV) shows evidence of *in vitro* and *in vivo* efficacy in human glioma xenografts and mouse syngeneic gliomas. It also shows reduced lethality when injected in the brains of susceptible mice without tumors. These results thus justify further exploration of NG34 in human GBM clinical trials.

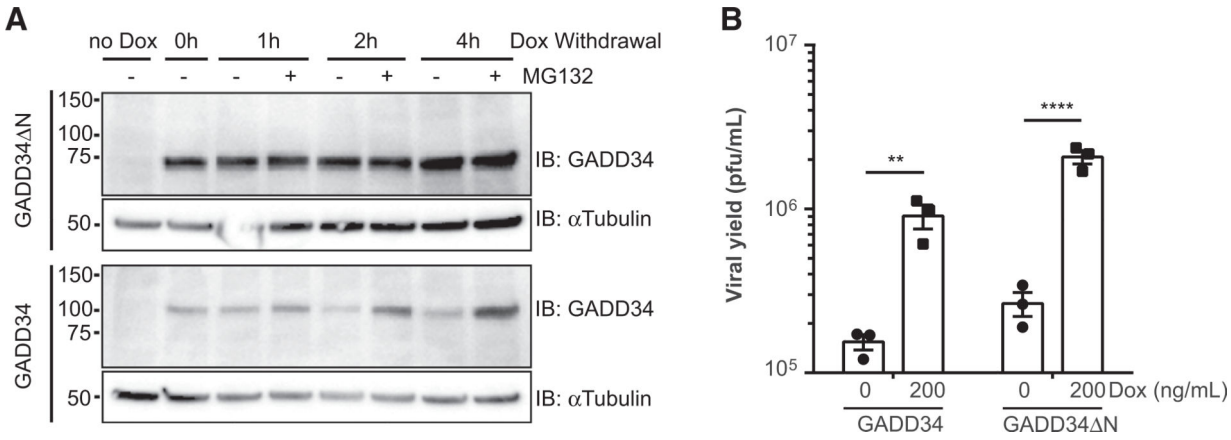

Figure 1.

GADD34 expression increases the viral yields of a γ34.5-null oHSV. **A,** Doxycycline (dox)-inducible GADD34 expressing U251 cells (designated as U251.G34) were treated with doxycycline (200 ng/mL) for 24 hours, followed by culture in the presence or absence of 20 μmol/L MG132 for the indicated times (0, 1, 2, and 4 hours). GADD34 and αTubulin were visualized by immunoblots (IB) utilizing the corresponding antibodies. Numbers on the left indicate molecular size (kDa). **B,** U251.G34 cells were infected by γ34.5-null rHSVQ virus at a multiplicity of infection (MOI) of 0.03 for three days in the presence or absence of doxycycline (200 ng/mL). Data represent the mean with SD of three replicates. Statistical analyses were conducted by Student *t* test, where ** indicates $P < 0.01$.

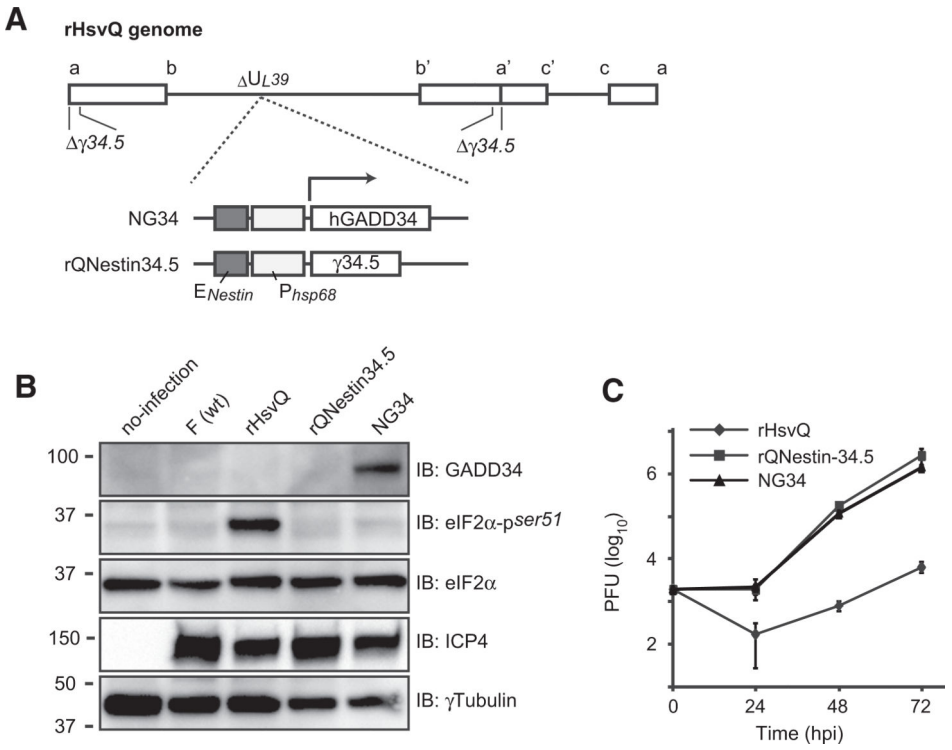

Figure 2.

Comparative phenotypic studies of GADD34-encoding NG34, γ34.5-null rHSVQ, and the γ34.5-encoding rQNestin34.5. **A,** Schematic maps of NG34 and rQNestin34.5 viral genomes. The human GADD34 (hGADD34) or viral γ34.5 gene are reengineered into the UL39 locus of the rHSVQ backbone (with diploid deletion of endogenous γ34.5 genes) in NG34 or rQNestin34.5, respectively. Both genes are controlled by regulatory elements of the nestin enhancer (E_{Nestin}) and hsp68 promoter (P_{hsp68}). The arrow indicates the longitudinal direction of transcripts. Rectangular boxes represent the inverted repeat sequence ab, bà', àc' and ca flanking the unique sequences. **B,** Immunoblots of GADD34, total and serine-51 phospho-eIF2α, viral ICP4 and γTubulin, using U251 cell lysates after 16-hour infection at MOI of 0.1 with the indicated oHSVs. **C,** Total viral yields assayed at the indicated time post infection with each oHSVs. Data represent the mean with SD of three replicates. Statistical analyses were conducted by two-way ANOVA followed by Dunnett multiple comparisons test against the rHSVQ group, where **** $P < 0.0001$ (vs. rQNestin34.5) and **** $P < 0.001$ (vs. NG34).

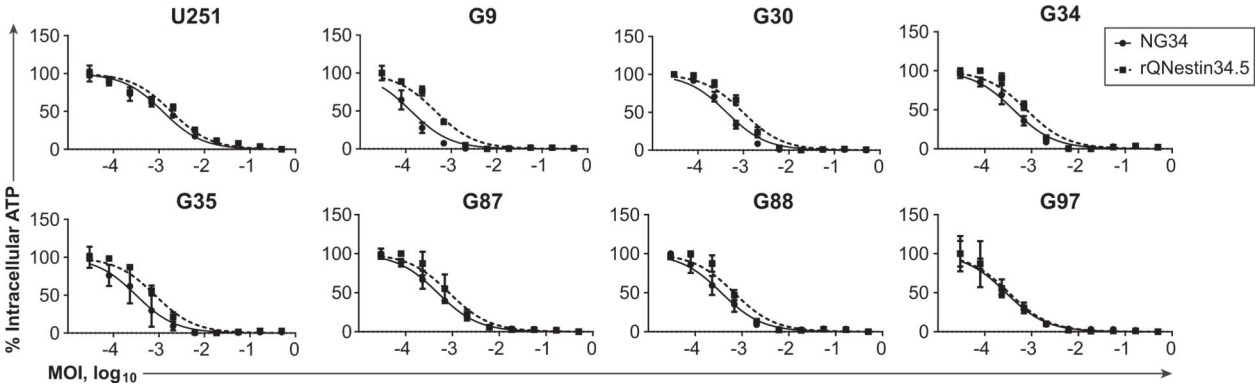

Figure 3.

Dose–response effects of human glioblastoma cells after the treatment with NG34 or rQNestin34.5. Intracellular ATP was measured as an index of cell viability, five days after infection of a GBM cell panel with NG34 or rQNestin34.5. Data were normalized with respect to maximum and minimum values before plotting the average value of four replicates with SD, error bars, and nonlinear dose–response curves. Ranges of 50% effective doses and values of R^2 at 95% confidence intervals are shown in Supplementary Table S1.

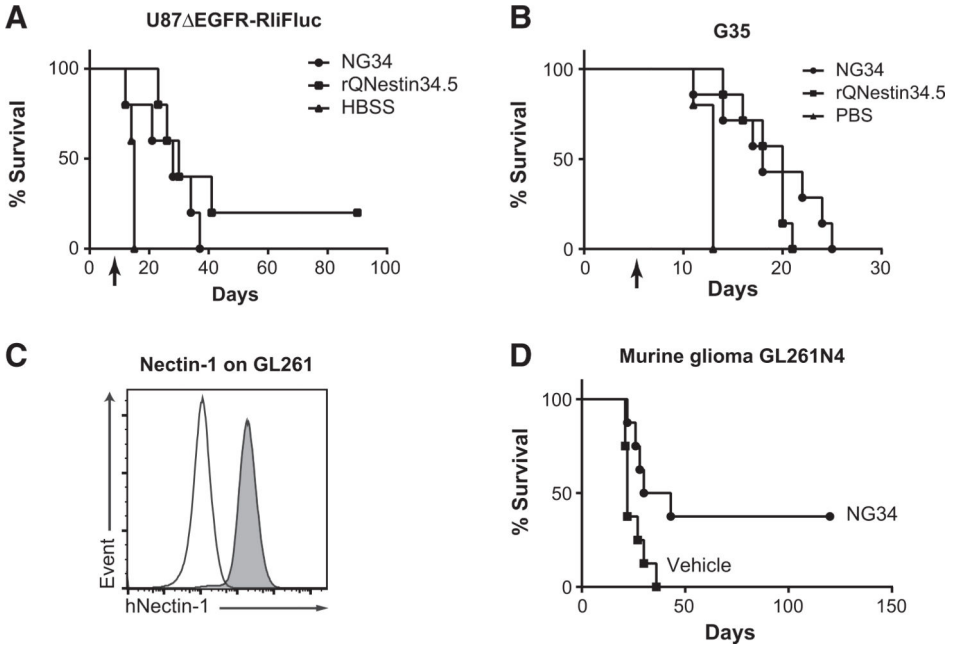

Figure 4.

Therapeutic efficacy of NG34 *in vivo*. **A** and **B,** Kaplan–Meier survival curves of athymic nude mice bearing intracerebral U87ΔEGFR-RliFluc (**A**) or G35 (**B**) GBMs after treatment with intratumoral oHSV (2×10^5 PFU) or HBSS vehicle on day 7 (**A**) or day 5 (**B**) postimplantation (U87ΔEGFR-RliFluc, $n = 5$; G35, $n = 7$) denoted by the arrow. Statistical analysis of (**A**) by log-rank test, where $P < 0.05$ (**A** and **B**), HBSS versus NG34; $P < 0.01$ (**A**) and $P < 0.001$ (**B**), HBSS versus rQNestin34.5; $P = 0.275$ (**A**) and $P = 0.392$ (**B**), NG34 versus rQNestin34.5. Tumor growth of U87ΔEGFR-RliFluc was also monitored by *in vivo* bioluminescence imaging as shown in Supplementary Fig. S4. **C,** Histograms showing the levels of human Nectin-1 expression (*y*-axis) on GL261 (white) and GL261N4 (gray) cells by FACS analysis using anti-human Nectin-1/CD111 antibody. **D**, Kaplan–Meier survival curves of C57Bl/6 mice bearing intracerebral murine GL261N4 glioma after treatment with intratumoral NG34 (1×10^6 PFU) or HBSS vehicle on day 7. Statistical analysis ($n = 8$, each) by log-rank test, where $P < 0.05$.

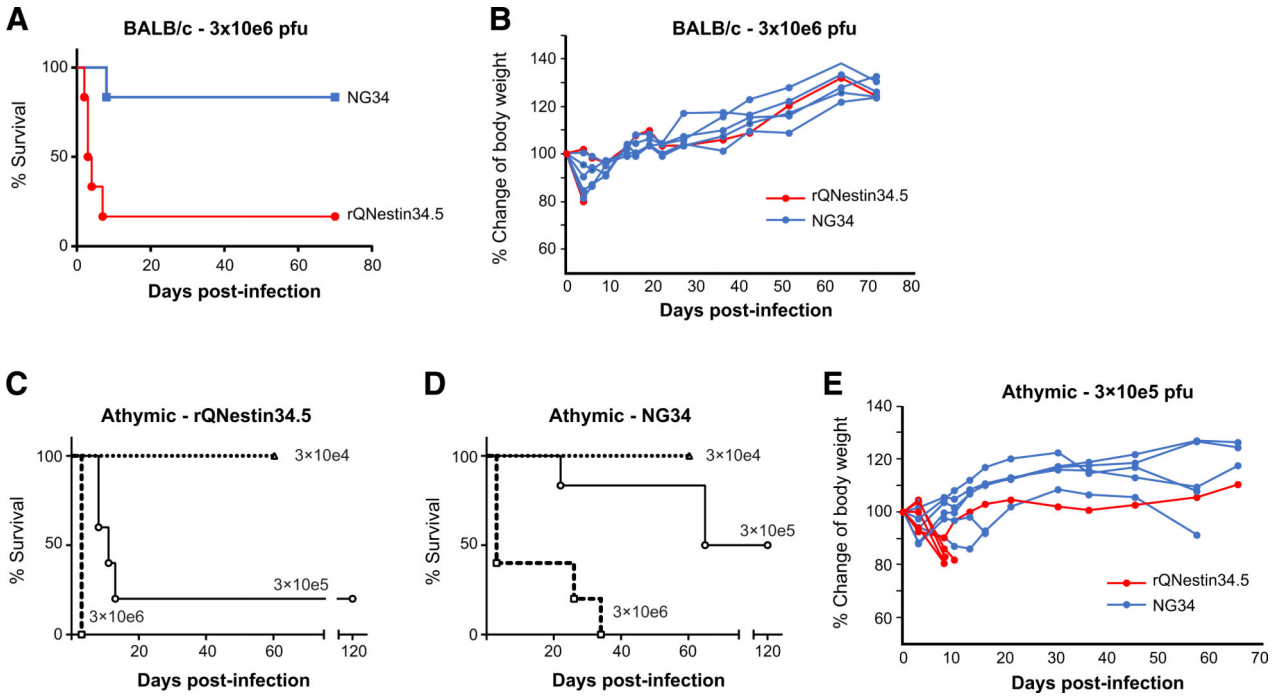

Figure 5.

Decreased mortality after intracerebral injection of NG34 versus rQNestin34.5. **A–D,** Survival of BALB/c (**A**) and athymic nude mice (**C** and **D**) inoculated intracerebrally with 3 × 10^6 pfu (**A** and **B**) or three different doses of either rQNestin34.5 (**C**) or NG34 (**D**). Kaplan–Meier survival curves were analyzed with Gehan–Breslow–Wilcoxon test, where $P < 0.001$ (**A**) and $P < 0.05$ (3 × 10^5 pfu of rQNestin344.5 in **C** and NG34 in **D**). Triangle with dot line; 3 × 10^4 pfu, circle; 3 × 10^5 pfu, and square with dot line; 3 × 10^6 pfu. Body weights of individual animals were also plotted in **B** (BALB/c; with doses of 3 × 10^6 pfu) and **E** (athymic; with doses of 3 × 10^5 pfu).

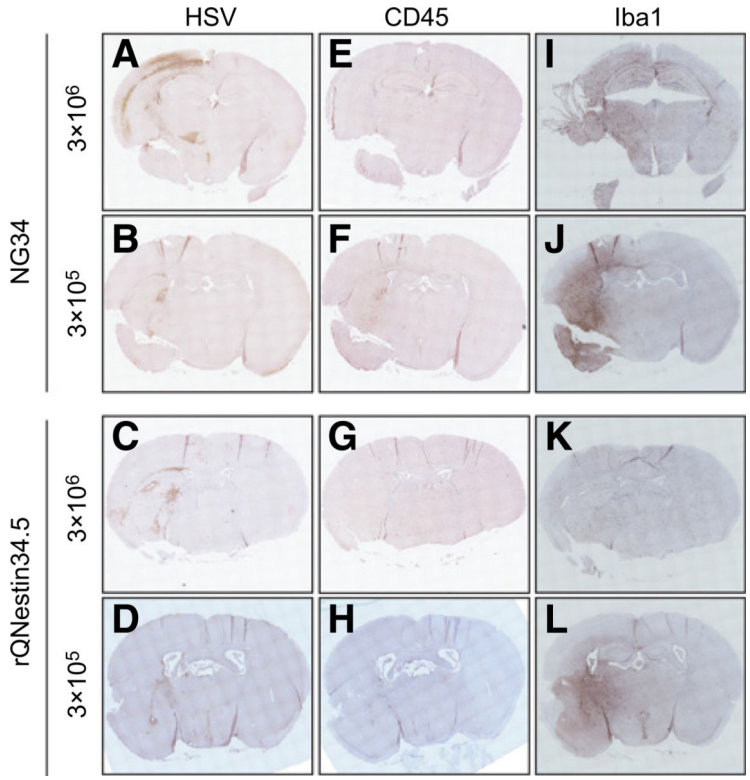

Figure 6.

IHC of the brains of athymic mice after the HSV-1 inoculation. Brains with 3×10^6 pfu were obtained from the euthanized mice at a terminal point (day 3) during the toxicity study in Fig. 5C and **D**. Brains with the 3×10^5 pfu were independently prepared for this study and obtained from the mice at day 5 after viral injection. The sections from the paraffin-embedded tissues were stained with anti-HSV1/2 (**A–D**), anti-CD45 (**E–H**), or anti-Iba1 (**I–L**) antibodies.

Table 1.

50% Effective dose of oHSV in GBM and non-GBM cell lines

MOI (×10^{-3}), 95% Confidence intervals				
	rHSVQ		NG34	
	ED50	R-Seq	ED50	R-Seq
U251	22.67 – 47.63	0.8947	2.620 – 5.436	0.8728
U2OS	15.11 – 41.57	0.7516	7.172 – 15.90	0.8516
G9Rluc	34.63 – 70.44	0.9173	4.827 – 7.922	0.9587
G30	9.439 – 16.87	0.9392	1.962 – 3.150	0.9588
G83	25.08 – 54.51	0.9028	4.424 – 9.737	0.8810
G326	17.87 – 43.33	0.8850	3.564 – 7.058	0.9237
G528	86.39 – 270.7	0.6973	26.66 – 64.31	0.8706

NOTE: Enhanced glioma cytotoxicity effect with GADD34-encoding γ1 34.5-null NG34 versus original γ1 34.5-null rHSVQ virus. Intracellular ATP was measured 3 days after oHSV infection with either rHSVQ or NG34 or rQNestin34.5 in GBM (U251, G9Rluc and G30) and non-GBM (U2OS) cells at 20,000 cells per a well of 96-well plates for cell viability assay. Data with three replicates were normalized with maximum and minimum values before calculating ranges of 50% effective doses (ED50) and values of R^2 at 95% confidence intervals. These plots with nonlinear dose–response curves are also provided in Supplementary Fig. S1.